JOURNAL OF RESEARCH of the National Bureau of Standards
Vol. 89, No. 1, January-February 1984

Impedance of a Coil in the Vicinity of a Crack

Arnold H. Kahn
National Bureau of Standards, Washington, DC 20234

Accepted: November 16, 1983

Calculations are presented for the impedance of a coil as it is moved in the vicinity of a v-groove crack in the surface of a metallic slab. The coil is modeled as a pair of parallel wires, oriented parallel to the crack, carrying equal and opposite currents. The inhomogeneous electromagnetic fields in the air above the slab and in the metal are determined by the boundary integral equation (BIE) method. This approach leads to a pair of coupled integral equations for the tangential components of the electric and magnetic field vectors on the surface of the slab containing the crack. The solutions, which are obtained by standard methods of discretization, are valid for arbitrary ratio of crack or coil dimensions to skin depth. Illustrations are presented of the Poynting vector distribution over the surface of the metal, including the crack faces. A plot of the complex impedance is given in the form of a coil scan across the crack.

Key words: boundary integral equations; crack detection; eddy currents; electromagnetic NDE; nondestructive evaluation.

1. Introduction

In the design of electromagnetic NDE systems for the detection and examination of cracks or other defects in conducting materials, it is necessary to have a quantitative description of the electric and magnetic fields in the vicinity of the defect. In practice, the fields are produced by an exciting coil, the impedance of which is used to provide the detection signal. (The voltage induced in a secondary pickup coil may also be used.) In previous work by the author [1,2][1], the fields in the vicinity of a crack were calculated for models based on excitation by a spatially uniform applied ac magnetic field such as would be found in the interior of a solenoid. The present work offers an improved description of the fields through the introduction of nonuniformity of the applied field due to finite coil size and the inclusion of coil position relative to the crack.

About the Author, Paper: Arnold H. Kahn, a physicist, is part of the Nondestructive Characterization Group in the NBS Metallurgy Division. The work on which he reports was supported in part by the NBS Office of Nondestructive Evaluation.

[1] Figures in brackets indicate literature references at the end of this paper.

Recently there has been significant activity in the development of theoretical modeling in electromagnetic NDE. The finite element method has been applied by Ida and Lord [3] to the cylindrical geometry of reactor tubing. Studies have been presented by Auld *et al.*, Kincaid *et al.*, Bahr, and others [4] on experimental and theoretical considerations of crack detection and coil design. A principal difficulty is the calculation of signals when the electromagnetic skin depth and crack size are of comparable magnitude, which is the domain of greatest sensitivity. The two-dimensional model of this paper represents a contribution toward the solution of this problem. A full three-dimensional treatment may be possible as new computing capabilities are developed [3].

2. Description of the Model and Theoretical Formulation

The calculations described in this paper are based on the following model: We consider a flat surface with an infinitely long, symmetrical v-groove representing a surface crack in a slab of metal. Below the surface, the material is homogeneous and uniform in conductivity. A pair of wires carrying equal and opposite currents is located above the slab and is oriented parallel to the crack. The wires are infinitesimal in thickness and infinite in extent. This

simplified model of an eddy-current testing configuration allows a two-dimensional calculation of the impedance signals due to the crack. The calculation will allow for the effect of crack dimensions; coil dimensions, elevation, and displacement; and the material parameters of the metal. This is an improvement over calculations in which the exciting field is spatially uniform.

By solving for the electromagnetic fields first on the surface of the metal and then at the exciting wires, we obtain the impedance due to the presence of the metallic region. If the problem is solved for a plane surface without the crack, then the additional impedance due to the crack may be obtained by subtraction. Also, by solving for different positions of the wires representing the detection coils, we may obtain the impedance signal on traversing the crack and also the signal due to liftoff effects.

The model is illustrated in figure 1. The circles above the surface represent the wires, with + and − indicating the direction of the impressed current $I_0 e^{-i\omega t}$, where ω is the angular frequency and t the time. The current is held at fixed amplitude I_0, according to the usual procedure for eddy-current NDE. In the figure additional parameters are shown: A is the separation between the wires, H is the height of the coil above the plane, P is the center position of the coil relative to the crack, D is the depth of the crack, and F is the half-width of the crack opening.

Because of the symmetry of this two-dimensional model, the electric and magnetic fields may be derived from a vector potential, **A**, which has only one component, A_z [5], where the z-direction is parallel to the wires and the crack. If the wires were not parallel to the crack, a full three-dimensional analysis would be necessary. The vector potential is thus of the form $A(x,y)e^{-i\omega t}$, where A is complex to represent phase relations with respect to the exciting current.

In the region above the conductor the vector potential satisfies a Helmholtz equation. However, at the frequencies of eddy current testing the transit time for wave propagation across the region of the crack is negligibly small and a quasi-static approximation is satisfactory. Thus, in the region above the metal slab the vector potential satisfies the Laplace equation,

$$\nabla^2 A = 0, \tag{1}$$

except for the singularities at the wires. Below the surface, in the metallic region, the Helmholtz equation is obeyed,

$$(\nabla^2 + k^2)A = 0, \tag{2}$$

where

$$k^2 = i\sigma\omega\mu \tag{3}$$

is the square of the propagation constant, σ is the electrical conductivity, and μ is the magnetic permeability. Here too, displacement currents are neglected, in this case because the ohmic currents represented by the k^2 term are so much larger. At the boundary surface, including the faces of the crack, the

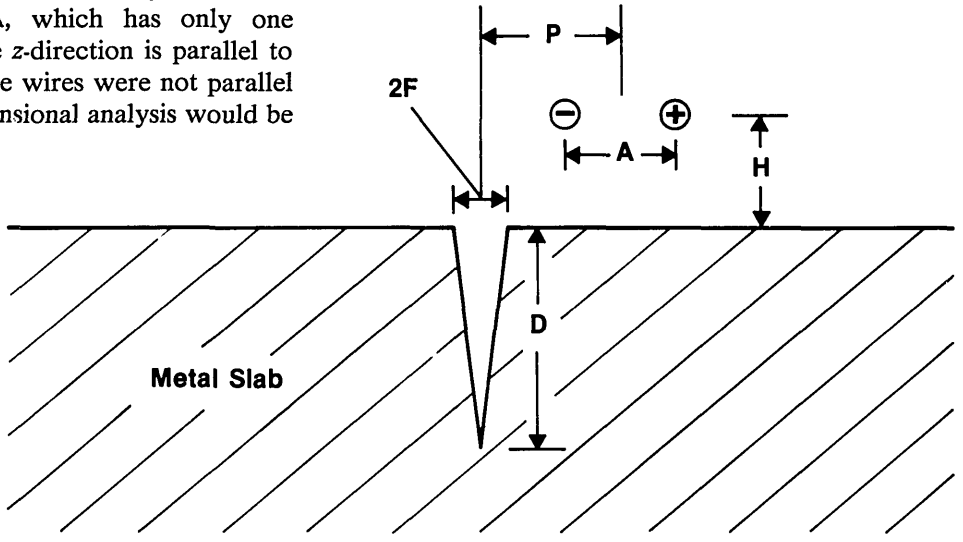

Figure 1–Configuration of model and parameters for the calculation of the impedance signal due to a crack.

D Crack Depth
2F Crack Opening
A Wire Separation
H Wire Elevation
P Wire Position Relative to Crack

usual conditions of continuity of tangential E and H, and normal B and D must hold. In terms of the vector potential, these conditions are equivalent to the continuity of A and $1/\mu\ \partial A/\partial n$, where $\partial A/\partial n$ is the normal derivative of A at the interface. To summarize, the vector potential must satisfy the Laplace equation in the upper region, the Helmholtz in the lower region, and conditions of continuity at the interface, and it must approach the known form of the impressed field in the vicinity of the source wires.

The method of solution selected in this paper is an extension of the boundary integral equation (BIE) approach [6,7]. This method, usually applied to a single region, has been used by the author [2] in eddy-current problems involving excitation by a uniform ac field. In the present application the method leads to a pair of coupled Fredholm integral equations of the first kind, as follows:

By application of Green's theorem we express the vector potential in the upper region in terms of the source fields and the values of A and its normal derivative $\partial A/\partial n$ on the bounding curve:

$$A(r)=\mathscr{S}(r)+\int\frac{\partial G(r,S')}{\partial n'}A(S')dS' - \int G(r,S')\frac{\partial A(S')}{\partial n'}dS'. \tag{4}$$

in which dS' is an element of arc in a planar cross-section normal to the surface of the metal. In the above, $\mathscr{S}$ is the vector potential due to the source wires as if the metallic region were absent. The two integrals give the change due to the induced currents below the boundary. They are taken over the boundary $\hat{\mathbf{n}}$ is the unit normal vector pointing out of the upper region. The remaining boundary closure at infinity makes no contribution since the fields decay with sufficient rapidity. Green's function for the Laplace operator is given by

$$G(r,r')=-1/2\pi\ \log|r-r'|; \tag{5}$$

it satisfies

$$\nabla^2 G(r,r')=-\delta(r-r'), \tag{6}$$

where δ is the two-dimensional Dirac delta function. For the two-wire case treated in this paper, the source field S has the form

$$S(r)=I_0[G(r,r_+)-G(r,r_-)],$$

where r_+ and r_- are the positions of the wires which carry the exciting current, I_0, parallel and anti-parallel to the z-direction, respectively. In the metallic region

$$A(r)=-\int\frac{\partial\mathscr{G}}{\partial n'}(r,S')A(S')dS' + \int\mathscr{G}(r,S')\frac{\partial A(S')}{\partial n'}dS', \tag{7}$$

where $\mathscr{G}$ is now the two-dimensional Helmholtz Green's function,

$$\mathscr{G}(r,r')=(i/4)H_0^{(1)}(k|r-r'|), \tag{8}$$

where $H_0^{(1)}$ is the Hankel function of the first kind, order zero. It, too, has a logarithmic singularity and satisfies the Helmholtz equation with a source,

$$(\nabla^2+k^2)\ \mathscr{G}(r,r')=-\delta(r-r'). \tag{9}$$

This latter Green's function contains the complex k and represents a damped outgoing cylindrical wave at large values of $r-r'$. In eq (7) we have retained the same direction of the normal vector $\hat{\mathbf{n}}$; hence the unusual sign convention on the right hand side.

The BIE method prescribes letting r approach the surface to obtain the fields on the bounding surface. When we let $r=S$, a well-defined expression is obtained if we use the Cauchy principal values for the singular integrals and replace A on the boundary by $A/2$. For nonmagnetic materials A and $\partial A/\partial n$ are both continuous across the boundary, and we shall so restrict the present calculations. The resulting BIE's are

$$\tfrac{1}{2}A(S)-\int\frac{\partial G(S,S')}{\partial n'}A(S')dS' + \int G(S,S')\frac{\partial A(S')}{\partial n'}dS'=\mathscr{S}(S) \tag{10}$$

$$\tfrac{1}{2}A(S)+\int\frac{\partial\mathscr{G}}{\partial n'}(S,S')A(S')dS' - \int\mathscr{G}(S,S')\frac{\partial A(S')}{\partial n'}dS'=0 \tag{11}$$

This is a coupled pair of equations for unknowns $A(S)$ and $\partial A(S)/\partial n$ on the interface. We may look on the

inhomogeneous term $\mathcal{S}(S)$ as the driving force for the system. When A and $\partial A/\partial n$ are found on the boundary, then the field A may be constructed at any point above the interface by application of eq (4), or below the interface by application of eq (7).

The ultimate objective is the determination of the impedance per unit length induced in the wires by the presence of the metallic region. The time-average of the power per unit length delivered by the exciting wires is given by the complex expression

$$P=\tfrac{1}{2}\int E'\cdot J^* da,$$

where J is the (constant) current density in the wires, E' is the electric field at the wires produced by the induced currents, and da is an element of cross-sectional area normal to the wires. E' is derived from the vector potential A' of the induced currents,

$$A'=A-\mathcal{S},$$

by the usual relation

$$E'=i\omega A'.$$

Hence, for a set of idealized line-wires, denumerated by the index i, we have

$$P=\tfrac{1}{2}\Sigma I_i^* i\omega A_i'.$$

Connection with conventional circuit parameters can be made by expressing P in terms of the currents, voltages per unit length, and impedance per unit length of the wires. Under the constant current assumption of eddy current testing, we have

$$P=\tfrac{1}{2}\Sigma V_i' I_i^*=\tfrac{1}{2}\Sigma I_i I_i^* Z_i,$$

where V_i' is the voltage per unit length induced in the ith wire and Z_i is the extra impedance in the ith wire due to induced currents in the metallic region. Finally we obtain

$$Z_i=i\omega A_i'/I_i$$

for the impedance per unit length in the ith wire, caused by the induction. Now A_i is evaluated at the ith wire and can be computed by use of Green's theorem after A and $\partial A/\partial n$ have been found on the interface. Thus we have a method of computing the extra impedance seen by each wire due to the presence of the metal below. These impedances may now be calculated with and without a crack being present.

3. Numerical Treatment

The coupled integral equations are solved by an application of the method of moments [8]. The solution is expressed as a linear combination of a finite set of basis functions with unknown coefficients. The coefficients are determined by requiring that the integral equations be satisfied at a number of points equal to the number of unknown coefficients; i.e., point-matching is used.

For the basis functions, the elements F shown in figure 2 were used, after the method of Harrington [8].

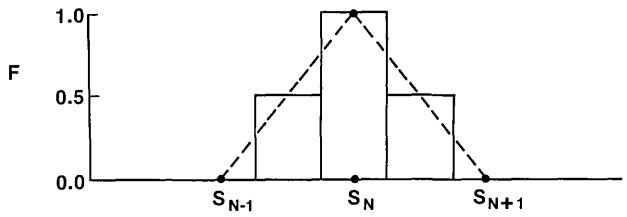

Figure 2–Triple-pulse hat function F used in the numerical calculations. The illustration shows the function $F(S-S_n)$. The dashed line is the common triangular hat-function.

We approximate the solution for the vector potential and its normal derivative on the interface by the finite sums:

$$A(S)=\Sigma A_i F(S-S_i) \tag{12}$$

and

$$\frac{\partial A(S)}{\partial n}=\Sigma N_i F(S-S_i) \tag{13}$$

These expansions are introduced into the integral equations, eqs (10) and (11). The integration over each element is carried out by use of the midpoint rule for the entire integrand of each flat section of the fundamental element, except when the Green's function is singular, i.e., when $S_i=S_j$.

When a singular integrand occurs in the evaluation of eq (10), the integration of the logarithmic Green's function is performed exactly. When a singular integrand occurs in eq (11), the dominant logarithmic part of the Hankel function is used for the evaluation.

The width of the elements is not restricted. It was found practical to use a fine grid where the solution

was large or varying rapidly, and a coarse grid elsewhere. With these approximations and the point-matching, the coupled integral equations are reduced to a linear algebraic system of the form:

$$\sum \left[\tfrac{1}{2}\delta_{ij} - \left(\frac{\partial G}{\partial n}\right)_{ij}\right] A_j + \sum G_{ij} \left(\frac{\partial A}{\partial n}\right)_j = \mathscr{S}_i \qquad (14)$$

$$\sum \left[\tfrac{1}{2}\delta_{ij} + \left(\frac{\partial G}{\partial n}\right)_{ij}\right] A_j - \sum \mathscr{G}_{ij} \left(\frac{\partial A}{\partial n}\right)_j = 0 \qquad (15)$$

In these equations, each doubly-subscripted term corresponds to that part of the integrations of eqs (10) and (11) connecting element j and matching-point i.

The calculations were first attempted with square pulse functions as the basis set. It was found that the solutions were unstable in the vicinity of the crack corners and near the location of a grid-size change. The use of the triple pulse element is equivalent to doubling the number of points in a pulse function calculation, but applying the constraint that the solution at each point be averaged with its two nearest neighbors. In addition to reducing the dimensions of the needed matrices, this has a smoothing effect and leads to solutions which are stable as the grid size is decreased. The triple pulse basis function may be looked upon as an approximation to the common triangular hat-function, shown in figure 2 by the dashed line. The hat-function yields a piecewise trapezoidal approximation to the solution which would be superior to the present form, but its application is precluded because of nonintegrability when multiplied by the Hankel functions of the integrand. The solution of the linear equations was obtained by Gaussian elimination without pivoting. The logarithmic singularities of the Green's functions associated with the diagonal elements of the matrices allow this economical simplification. The solutions were considered to have converged when further refinement produced an insignificant change in the physical results, usually about 1 percent. Typically the dimension of the square matrices ranged from 200 to 300.

4. Coil Impedance in the Absence of a Crack

The radiation field of an oscillating dipole above a conducting earth was a problem first attacked successfully by Sommerfeld [9]. Analytical solutions have been given for finite coils by Dodd *et al.* [10,11]. These solutions are in the form of integrals over various Bessel function arguments. Numerical evaluation is possible; analytic evaluation is in terms of asymptotic series. The same methods can be applied to this problem of a pair of parallel wires over a plane. However, the approach of this publication is readily applicable in the absence of a crack. Solving an integral equation requires a greater computing effort than evaluating an integral solution for the lesser problem. However, it is quite useful to have the programs available as a byproduct of the crack case. In this section we examine the results of calculations for the parallel wire coil above a flat conducting half-space, calculated by the boundary integral equation method.

In figure 3 we show the results of a typical calculation. For this case, and all others reported here,

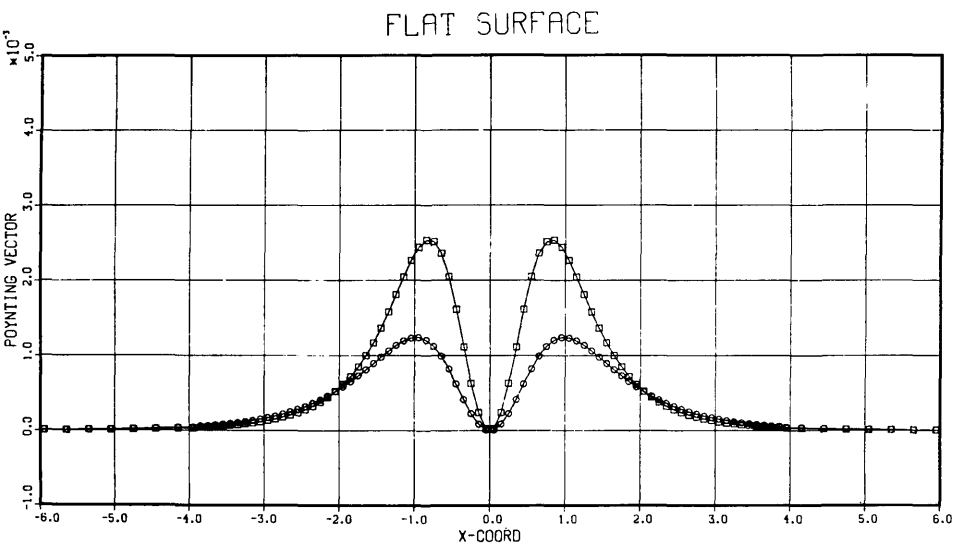

Figure 3–Poynting vector on the surface of a metallic slab in the absence of a crack. The coordinate x is along the flat surface of the metal. Distances are in units of the skin-depth and the Poynting vector is in units of $\mu_0\omega\ 10^{-3}$. The exciting wires are located at $\pm 0.5\ \delta$ and are at an elevation of $0.5\ \delta$.

lengths are in units of the skin depth δ, where

$$\delta = \sqrt{2/\sigma\omega\mu_0}, \tag{16}$$

and the symbols under the radical are the same as before. The complex Poynting vector $\bar{\mathbf{S}}$, represents the time average of the complex energy flux, in our application, across the surface of the conductor. In the units we are using, we have

$$\bar{\mathbf{S}} = \tfrac{1}{2}E \times H^* = -\frac{i}{2}\frac{\mu_0\omega}{\delta}\left|I_0\right|^2 A\frac{\partial A^*}{\partial n'}, \tag{17}$$

where A and $\partial A/\partial n'$ are calculated by solving the coupled boundary integral equations. While our principal interest is in the impedance change of the exciting wires, the Poynting vector plots show a detailed picture of the radiation field. The plots are useful for assessing the convergence of the calculations as well as for showing the regions of the test material where the significant absorption and field penetration take place.

5. Coil Impedance With a Crack

The presence of the crack adds two more parameters to the required inputs to the calculation. We treat only a symmetric v-groove crack which we specify by its depth and the half-width at its mouth. The calculations are performed in the same way as without the crack, with the only difference being that the needed matrices are larger in dimension and somewhat more complex in preparation. The algorithms for the solution are identical to those of the previous case. The output of the program is the impedance per unit length of the wires, with the crack present. In addition we may inspect the complex Poynting vector on the surface of the crack as well as on the flat surface of the test material.

For the initial investigations we selected a crack depth of 2.0 δ and an opening of half-width 0.25 δ. The coil wires were taken as having a separation of 1.0 δ and at an elevation of 1.0 δ above the plane. These dimensions correspond to the physical situation of a No. 30 AWG wire insulated pair in close contact, elevated one radius above the contact with the plane, and driven at a frequency of 110 kHz. The relevant parameters for this model applied to aluminum are given in table 1.

Table 1. Parameters for model calculation based on aluminum at 110 kHz.

Resistivity	ρ	2.82×10^{-8} Ω·m(20 °C)
Conductivity	$\sigma(=1/\rho)$	3.54×10^{7} $\Omega^{-1}m^{-1}$
Skin depth	δ	0.255 mm
Crack depth (=2δ)		0.51 mm
Crack half-opening (δ/4)		0.064 mm
Wire radius (δ/2)		0.13 mm

The calculations were performed for a range of values of the parameter P, the location of the coil center relative to the crack. Figures 4, 5, and 6 show the Poynting vector for the values P=2.5 δ, 0.5 δ, and 0.0

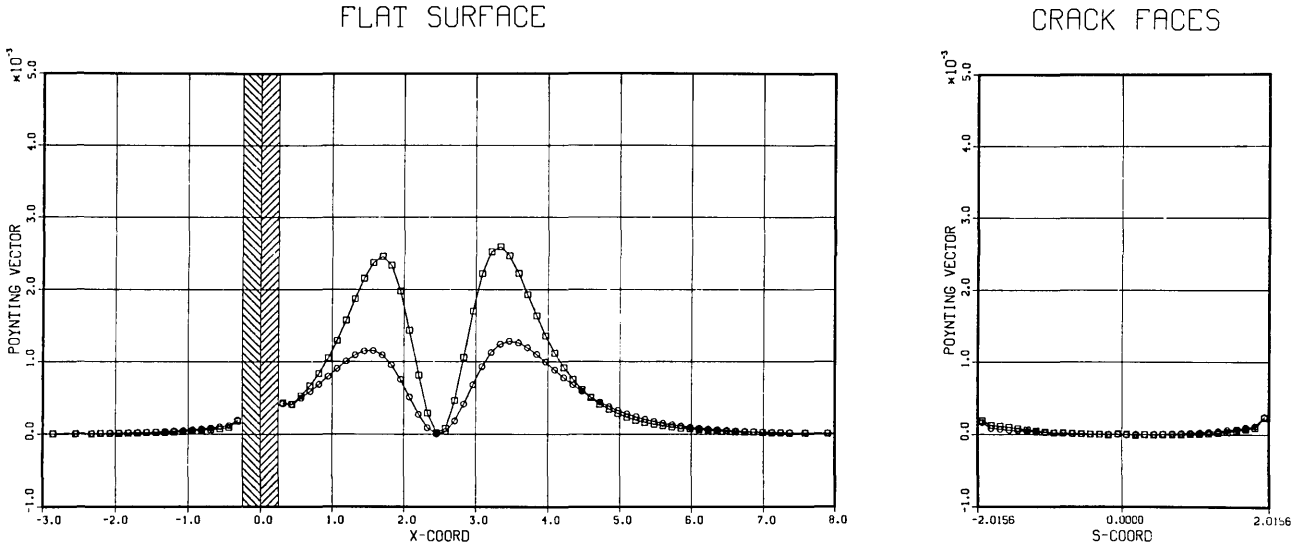

Figure 4–Poynting vector on the surface of a metallic slab with a crack. The coordinate S is along the faces of the crack, which is shown as folded open in the right-hand figure. The shaded band indicates the location of the v-groove crack. The lateral distance between the coil and the crack, P, is 2.0 δ and the half-opening, F, is 0.25 δ. All other parameters are as in figure 3.

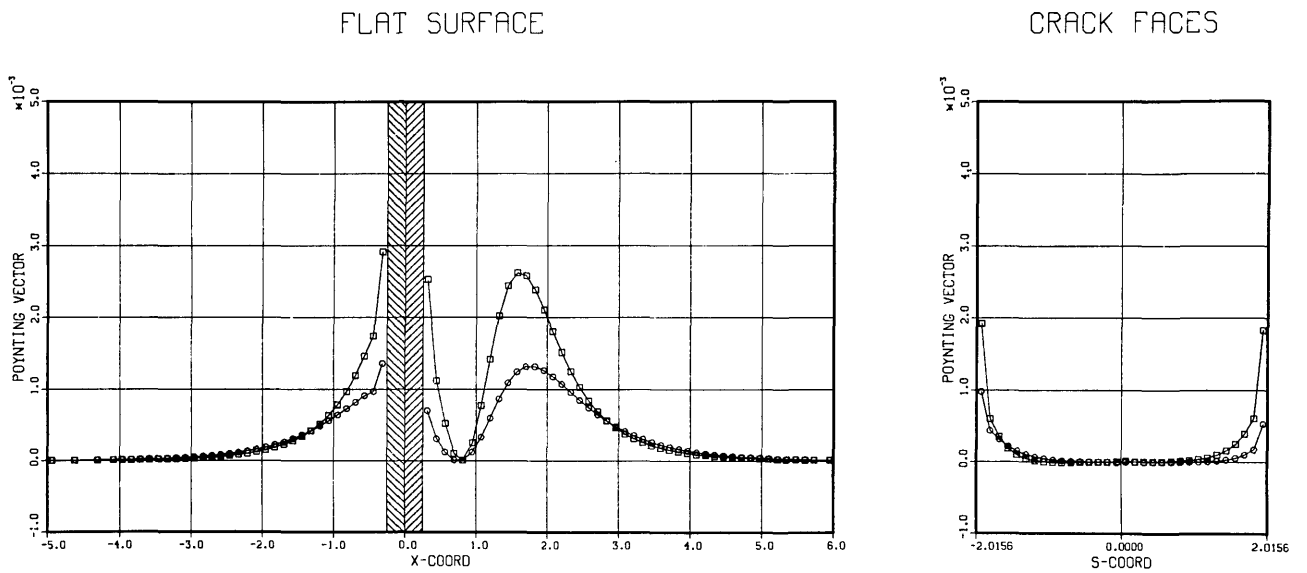

Figure 5–Poynting vector on the surface of a metallic slab with a crack. The lateral distance between the coil and the crack, P, has the value of 0.80 δ; all other parameters are as in figure 4.

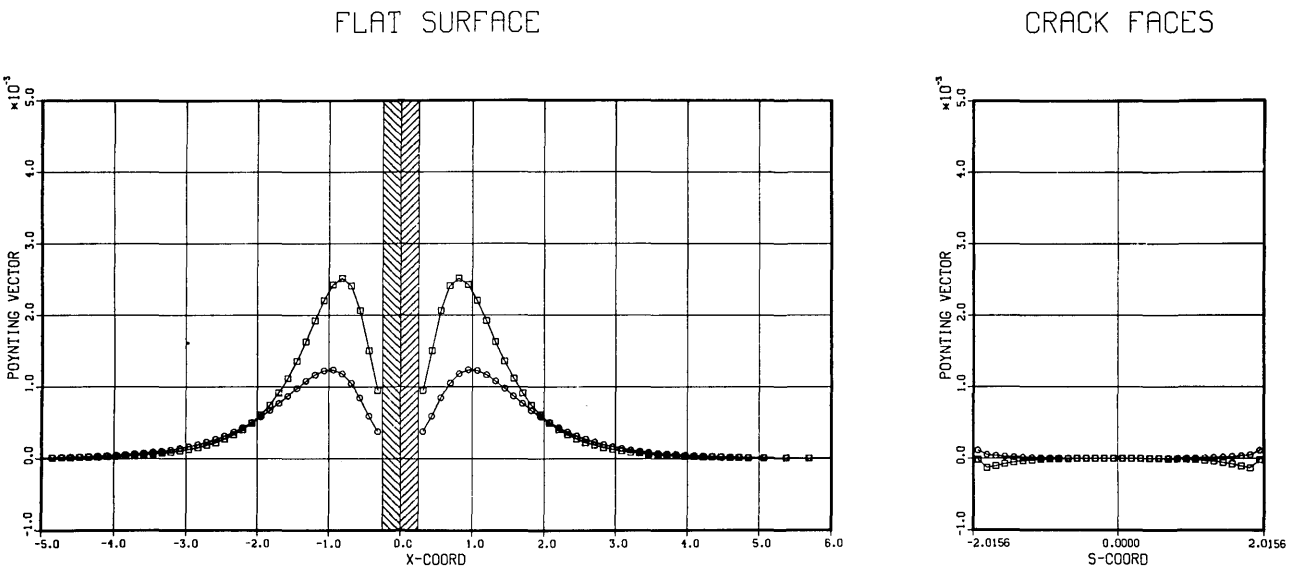

Figure 6–Poynting vector on the surface of a metallic slab with a crack. The lateral distance between the coil and the crack, P, has the value 0.0 δ; all other parameters are as in figure 4.

δ respectively, illustrating the deformation of the fields as the coil is brought up to the crack. These figures correspond to the same wire separation and elevation as in figure 3, the case with no crack.

Qualitative examination of the figures shows that in the presence of a crack, a portion of the integrated Poynting flux is "stolen" from the nearer of the peaks in the field distribution. The Poynting flux at the corners is somewhat increased over the value that would occur at that position if no crack were present. Inside the crack, the Poynting flux decays to zero in approximately one skin-depth. This is quite the opposite behavior to that which occurs in the case of a uniform H-field parallel to the crack [2]. In that case, the Poynting vector is greatest at the tip and vanishes at the corners.

From a series of calculations like these, the coil impedance per unit length was obtained for numerous positions of the coil. The phase and magnitude of the impedance are shown in the plots of figure 7, in the

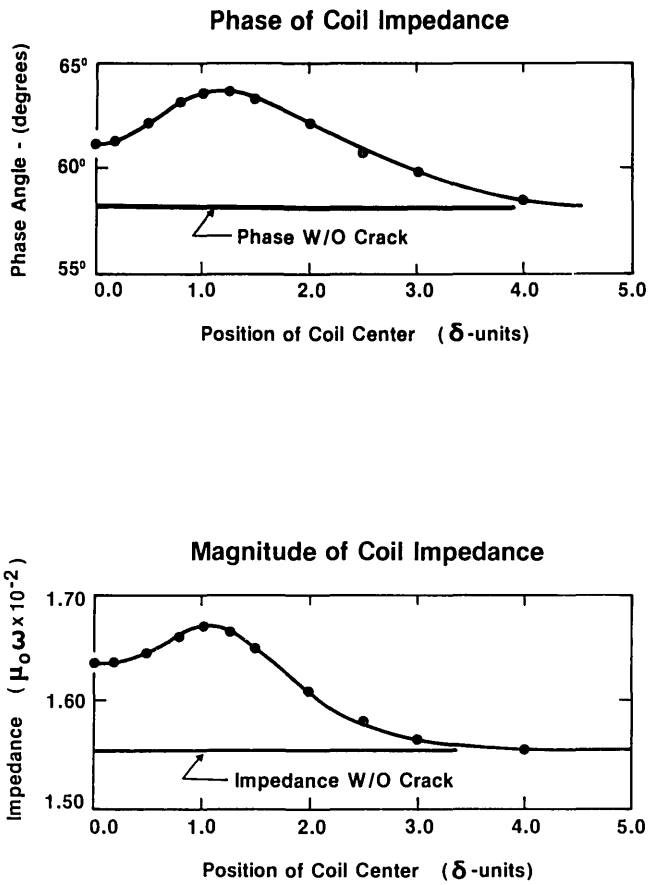

Figure 7–Plots of the phase and magnitude of the crack impedance signal as a function of the lateral displacement of the coil center relative to the crack. Parameters are as in figure 4.

form of a scan across the surface of the slab. These curves would be extended symmetrically for negative values of the coil displacement. The asymmetric signal obtained from an opposed pair of coils [12] can be obtained from these curves by computing a differential scan corresponding to the coil pair separation.

The author wishes to express his thanks to Dr. B. Auld and Dr. C. Fortunko for most valuable discussions concerning crack detection. He is also grateful to Dr. S. Gershovits for interesting suggestions.

References

[1] Kahn, A. H.; Spal, R.; Feldman, A. J. Appl. Phys. **48**, 4454 (1977).

[2] Kahn, A. H. in *Review of Progress in Quantitative Nondestructive Evaluation* 1, D. O. Thompson and D. E. Chimenti, eds., Plenum Press, New York, NY, p. 369.

[3] Ida, N.; Lord, W. IEEE Computer Graphics and Appl. **3**, 21 (1983).

[4] *Review of Progress in Quantitative Nondestructive Evaluation* 2, D. O. Thompson and D. E. Chimenti, eds., (1983).

[5] Landau, L. D.; Lifshitz, E. M. *Electrodynamics of Continuous Media*, Pergamon Press, New York, NY (1960), p. 121.

[6] Rizzo, F. J. in *The Boundary-Integral Equation Method: Computational Applications in Applied Mechanics*, T. A. Cruse and F. J. Rizzo, eds., American Society of Mechanical Engineers, 1975, p. 1.

[7] Jaswon, M. A.; Symm, G. T. *Integral Equation Methods in Potential Theory and Electrostatics*,, Academic Press, London (1977).

[8] Harrington, R. F. *Field Computation by Moment Methods*, Macmillan, New York, NY (1968).

[9] Sommerfeld, A. *Partial Differential Equations in Physics*, Academic Press, New York, NY (1949), p. 236 *et seq.*

[10] Dodd, C. V.; Deeds, W. E. J. Appl. Phys. **39**, 2829 (1968).

[11] Dodd, C. V.; Deeds, W. E.; Luquire, J. W. Int. J. Nondestructive Testing **1**, 29 (1969).

[12] Fortunko, C. M.; Padget, S. A. Technical Activities 1982, Office of Nondestructive Evaluation, NBSIR 82-2617, p. 57 *et seq.*